Open access • Proceedings Article • DOI:10.1109/WIMOB.2016.7763261

Studying the impact of LTE-U on Wi-Fi downlink performance — Source link

Amr Abdelfattah, Naceur Malouch

Institutions: University of Paris

Published on: 01 Oct 2016 - Wireless and Mobile Computing, Networking and Communications

Topics: Spectrum management, LTE in unlicensed spectrum and 5G

Studying the Impact of LTE-U on Wi-Fi Downlink Performance

Amr Abdelfattah
Sorbonne Universités, UPMC Univ Paris 06
CNRS, LIP6 UMR 7606
4 place Jussieu 75005 Paris
Email: amr.abdelfattah@lip6.fr

Naceur Malouch
Sorbonne Universités, UPMC Univ Paris 06
CNRS, LIP6 UMR 7606
4 place Jussieu 75005 Paris
Email: naceur.malouch@lip6.fr

***Abstract*—To address the mobile data growth challenges, mobile operators need to access more spectrum resources. LTE in unlicensed spectrum (LTE-U) has been proposed to extend the usual operation of LTE in licensed spectrum to cover also unlicensed spectrum, mainly at 5 GHz band due to its wide spectrum availability. However, this extension poses significant challenges especially regarding the coexistence between LTE-U and legacy systems like Wi-Fi. In case of LTE-U adopts Time-Division Multiplexing (TDM) schemes to share the spectrum with Wi-Fi, we expect performance degradations of Wi-Fi networks. In this paper, we quantify the impact of TDM schemes on Wi-Fi performance in a coexistence scenario. We provide an analytical model to compute the probability of collision faced by Wi-Fi and its downlink throughput performance. This model provides an upper bound of the probability of collision that could be faced by a finite number of Wi-Fi stations. NS3 simulations show that the model estimates accurately the collision probability and the throughput experienced by Wi-Fi. The model is then used to study and compare different coexistence schemes showing for instance that the Wi-Fi frame size impacts globally the performance of Wi-Fi users.**

***Index Terms*—LTE-U, Duty Cycled LTE, Wi-Fi, 5G, Mobile Communication, Collision Probability, Peformance Evaluation, Simulation.**

I. Introduction

According to Cisco forecast, by 2019, the monthly global mobile data traffic will exceed 24.3 Exabyte [1] because of the increasing number of mobile broadband data subscribers. This motivates mobile operators to increase the capacity of their cellular networks to cope with this challenge. As next-generation communication systems (i.e. LTE, LTE-A) performance is close to Shannon bound in terms of spectrum efficiency, cellular networks move towards data traffic offloading from licensed to unlicensed spectrum which stands out as a promising solution. One technique to perform offloading is to mix wireless technologies by using Wi-Fi networks as an alternative or as a complementary network for cellular networks. In heterogeneous networks, the user equipment accesses licensed and/or unlicensed spectrum to improve data throughput with the price of adding complexity to the network. Another technique is to extend the operation of LTE to unlicensed spectrum, called LTE in Unlicensed band (LTE-U), so that mobile operators have an easy and transparent usage of unlicensed spectrum in a unified network environment which typically promises higher spectral efficiency than Wi-Fi. Enabling LTE-U and Wi-Fi networks to operate in the same shared spectrum requires considering coexistence scenarios carefully. LTE-U has to adopt a spectrum sharing scheme to coexist fairly with Wi-Fi and fulfill telecommunication regulatory agencies requirements to occupy this spectrum.

In regions such as Europe, Japan and India, accessing unlicensed spectrum requires that LTE adopts a Listen Before Talk (LBT) spectrum sharing scheme with the so-called channel clear assessment (CCA) mechanism. To add this new flavor to LTE, we can exploit Load Base Equipment (LBE) or Frame Based Equipment (FBE) mechanisms defined in [2] as two options for LBT scheme. As a result, we expect a huge modification on LTE standard and losing backward-compatibility with latest standards. In a white paper published by Qualcomm [3], LTE-U has used an FBE mechanism to coexist with Wi-Fi in an outdoor simulation scenario. The simulation results show that LTE-U is a better neighbor to Wi-Fi than Wi-Fi to itself. However, [4] shows that when the load of LTE-U is very high, LBT impacts significantly the performance of Wi-Fi users while LTE-U users remain robust.

LBT adaptation prerequisite was dismissed for other regions such as USA, China and Korea. Therefore, an intuitive and simple way to share the spectrum is to prevent LTE-U and Wi-Fi from accessing the channel at the same time using Time-Division Multiplexing (TDM) schemes. LTE-U occupies the channel for some period of time then vacates it to allow Wi-Fi users to access it for some amount of time. To do so, LTE-U can choose either a short or a long TDM duty cycle dynamically or statically. TDM adaptation is compatible with existing LTE standards thanks to LTE advanced features. Hence, mobile operators can leverage the large LTE ecosystem. For instance, a key LTE feature called SCell activation/deactivation can be used to have a long TDM duty cycle where LTE-U and Wi-Fi access the channel in time across several milliseconds ($20 \sim 100$x ms). In [5], the authors propose a simple way to have a short TDM duty cycle ($1 \sim 10$ ms) over an LTE frame of 10 ms through a modified version of Almost Blank Subframes (ABS) feature where LTE reference signals had been totally removed to have blank subframes.

On one hand, TDM schemes allow better control on how and when the spectrum is accessed by LTE and Wi-Fi, and

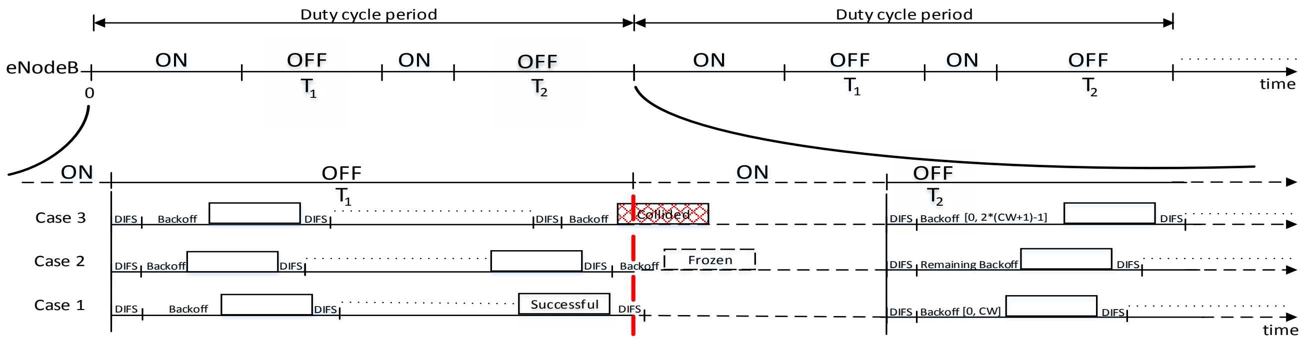

Fig. 1: LTE-U eNodeB interacting with Wi-Fi Access Point

thus master better the sharing. On the other hand, collisions with Wi-Fi may occur when LTE starts a transmission period after a silence period or after a blank subframe. In this paper, we aim at quantifying the impact of LTE TDM schemes on the performance of Wi-Fi networks at the MAC level by computing analytically the probability of collision. We model the interaction between LTE and Wi-Fi using both delayed and ordinary renewal processes associated with a stopping time directly related to LTE-U idle periods. We also use a discrete time Markov chain to model the progress of the interaction over time. We similarly compute the offered downlink throughput of a Wi-Fi access point. In addition, we have implemented the TDM scheme in the open-source NS3 (Network Simulator version 3) simulator [6] and we used its complete implementation of IEEE 802.11 standard to validate our model and assess its robustness when the model assumptions are not quite valid.

The previous work [7] has studied the LTE and Wi-Fi interaction through blank subframes in indoor environment for single and multiple-floor scenarios. Multiple TDM configurations have been examined using a proprietary semi-static system-level simulator. The results show first that the more the number of blank subframes over LTE frame, the higher the offered Wi-Fi throughput. Second, for the same number of blank subframes, Wi-Fi can experience different throughputs. These results were partially justified by the system-level simulator since the exact impact on the Wi-Fi performance was not analyzed. Thus, it is hard to compare between TDM schemes to find the best configuration parameters that maximize the throughput and reduce the collision probability. In this work, we provide a formal justification of the possible performance degradation experienced by Wi-Fi. We show how the Wi-Fi performance is related to the number of blank subframes during the LTE frame and also to their distribution along the frame. Through the model and supported by NS3 simulations, we show that the packet size has an important role to increase or decrease the Wi-Fi throughput especially for low Wi-Fi channel bit rates.

In [8], the authors found that for a fixed TDM duty cycle percentage, if the duty cycle period is too short, the throughput of Wi-Fi can be negatively impacted. However, if the duty cycle period is too long, it is more the packet latency that will be degraded. Our work complements these results by studying different duty cycle patterns while using a compromised duty cycle period.

Other coexistence techniques were also studied in the previous work. Chen *et al.* have studied in [4] the downlink performance of Wi-Fi when LBT scheme is deployed. They used a Markov chain to model Wi-Fi random access to the spectrum. [9], [5] have investigated spatial spectrum sharing in indoor environment where the objective is to separate away LTE and Wi-Fi devices to avoid interferences. In contrast, [10], [11] propose an interference-aware power control to share the spectrum with Wi-Fi. Our work complements these previous works by studying another coexistence approach especially that neither one of them have proved optimal efficiency in all network scenarios. Moreover, TDM schemes have the advantage of being more flexible and easy to deploy.

The paper is outlined as follows. In Section II, we explore the interaction between LTE-U and Wi-Fi. In Section III, we provide an analytical model for Wi-Fi coexisting with LTE-U to quantify the impact of LTE-U on an infrastructure-based Wi-Fi network in terms of probability of collision and saturation throughput. Section IV validates the accuracy of our model by comparing its results with those obtained by means of NS3 simulations. We investigate the performance of Wi-Fi in various TDM schemes and Wi-Fi configurations. Finally, conclusions and future work are drawn in Section V.

II. LTE-U eNodeB interacting with Wi-Fi Access Point

In this section, we explore the impact of LTE-U eNodeB transmissions on Wi-Fi downlink transmissions by an Access Point (AP) in infrastructure mode. The use of different MAC techniques by LTE-U and Wi-Fi creates a major sharing problem. By default, LTE-U does not sense the channel before transmitting to know whether it is idle or not unlike Wi-Fi which follows an LBT scheme. As a result, an unexpected interruption of Wi-Fi transmission by LTE-U can be produced at several times leading to the collision between the two systems.

In Figure 1, eNodeB is activated/deactivated during ON/OFF periods. This ON/OFF pattern is controlled by three different parameters. First, the duty cycle period that determines how long it takes to the pattern to be repeated again. Second, the duty cycle percentage which is the portion of time where the eNodeB is activated over the duty cycle period. Third, the transmission periods during the duty cycle period which controls how the eNodeB ON/OFF periods are distributed during the duty cycle. This transmission periods can be continuous or separated by several silence periods.

Now, we turn our attention to the periods where AP can access the channel corresponding to eNodeB-OFF periods. We look first at the end of these periods (See Figure 1). In each period, after a successful transmission of some frames, when the next eNodeB-ON period starts, it can start when Wi-Fi is sensing the channel during a DIFS which is the Distributed InterFrame Space (Case 1 in Figure 1). The eNodeB period can also start during the decrementing of the backoff counter of the Wi-Fi AP (Case 2). Effectively, after the DIFS sensing period, the Wi-Fi AP transmits its frame after a random number of slots called backoff time. Finally, the eNodeB period can start during the Wi-Fi frame transmission (Case 3).

To get into more details, in the first case, eNodeB interruption comes after the end of a frame transmission that is why the last frame is successfully transmitted. Then, AP defers the next transmission until the eNodeB transmission period is finished. Then, at the next Wi-Fi transmission period (eNodeB-OFF), a new frame will be transmitted after sensing the channel for a time equal to the DIFS and the slotted random backoff time period corresponding to a random backoff counter uniformly chosen in the range of [0, CW], where CW is the initial backoff contention window size. The backoff time is fully determined by this counter since the slot time is fixed. We denote the slot time by δ.

In the second case, the eNodeB interruption comes during the slotted random backoff time period while AP is decrementing its backoff counter at the end of each slot time δ. When AP senses the channel busy, it freezes the backoff counter and the frame transmission procedure is *frozen* until the next eNodeB-OFF period that is why we call the last frame is a frozen frame. At the next eNodeB-OFF period, the frozen frame is transmitted after sensing the channel again for a time equals to DIFS and after decrementing the rest of the frozen backoff counter from the previous period.

As for the third case, the eNodeB interruption comes during Wi-Fi frame transmission so a collision is occurred and the frame is lost for that reason we call the last frame is a collided frame. At the next eNodeB-OFF period, AP retransmits that collided frame again after a DIFS period and a uniform random backoff time with a doubled backoff contention window size equals to $2 * (CW + 1) - 1$.

III. Analytical Model

The analysis is divided into two steps. First, we study the behavior over time of the AP coexisting with eNodeB using a Discrete Time Markov Chain (DTMC). Second, we compute the transition probabilities by considering the Wi-Fi transmissions as a renewal process stopped by LTE-U arrival. Finally, we obtain the probability of collision under the saturation condition, and we express the AP downlink throughput.

Over a duty cycle period, AP can access the channel during different eNodeB-OFF time periods. Let us adopt the notation T_i for such periods where i $\in (1, \cdots, M)$ and M is the number of disjoint access channel opportunities offered to AP during a duty cycle period (see Figure 1 for M=2). As mentioned in Section II, we enumerated three cases where the AP transmission during any T_i period terminates with a frozen, collided or success frame, as shown in Figure 1. Thus, the end of each T_i period can be adequately modeled by means of a three-state Markov chain. Let us denote by $S = \{f_i, c_i, s_i\}$, the space state for period T_i, where f_i, c_i and s_i indicate that the AP transmission has been ended with a frozen, collided and success frame during T_i period respectively. As a result, any given T_i period has a set of three states which can be visited again *only* at multiples of M leading to a periodic DTMC with period M. This shown in Figure 2 for $M = 3$, i.e. periods T_1, T_2 and T_3. We should note also that the Markov chain can lose the periodicity when at least two periods of T_i periods have the same time values over the duty cycle period.

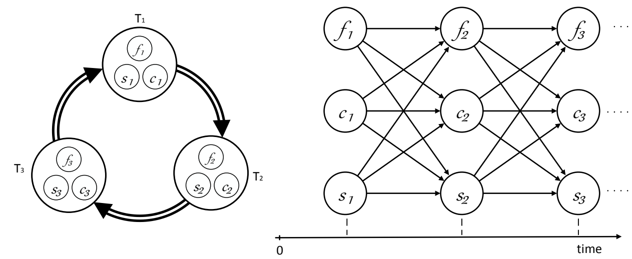

Fig. 2: Periodic Discrete Time Markov Chain modeling the three states at the end of an eNodeB-OFF period (T_i). Left: The global transition diagram showing the periodicity. Right: Detailed state transitions over time

In order to keep the Markov property, we assume that after a collision at the end of a T_i period, the retransmitted frame at the beginning of the next T_i period does not face a collision. To relax this assumption, we should add the current number of accumulated successive collisions in the Markov chain states which complexifies too much the model without a significant accuracy gain as we shall see later. Indeed, these T_i periods are multiples of 1 ms and thus they are relatively large compared to the AP frame transmission time. It is intuitive that this assumption is more valid as long as T_i period gets larger and AP frame size gets smaller. Besides, the high rates provided by recent Wi-Fi technologies allows several frame transmissions in 1 ms even for large packet sizes.

A. Transition Probabilities and Probability of Collision

In this subsection, we show how we can calculate the transition probabilities between any two states in our Markovian model using renewal processes. Then, we compute the global probability of collision faced by any AP frame transmission.

After the eNodeB transmission is finished, the AP starts immediately to transmit its frames at the beginning of a T_i period. As described in Section II, the amount of time needed for DCF protocol to successfully transmit the first frame depends on how ended the AP transmission during the previous period. The previous period is T_{i-1} for $i \in (2, \cdots, M)$, and T_M for $i = 1$. For simplicity of notation and without loss of generality, we denote by T_{i-1} the previous period for all i. First, let us consider that T_{i-1} period state was s_{i-1} (success). Then, the amount of time needed to successfully transmit the first frame at T_i period can be represented by the following uniform random variable:

$$X = DIFS + \delta * BFcounter_{unif(0,CW)} + Frame_{time} \quad (1)$$

Where $BFcounter_{unif(0,CW)}$ is the backoff counter which is a uniform random variable with lower and upper limits of 0 and CW respectively. $Frame_{time}$ is the frame transmission time which includes the frame airtime over the channel, followed by a period of time equals to Short InterFrame Space (SIFS) and the acknowledgment transmission time (Acktime). That is $Frame_{time}$ = frame airtime + SIFS + Acktime. We compute frame airtime and Acktime to account for different OFDM physical layer as in [12].

Now, consider that T_{i-1} period state was f_{i-1} (frozen), then the first frame at T_i period will be transmitted after a $DIFS$ time plus the remaining time of the frozen backoff period. The probability mass function (pmf) of the remaining number of time slots of the frozen backoff counter depends on when the last eNodeB-ON transmission period has been started during the last slotted random backoff at T_{i-1} period. Whereas the remaining backoff counter random variable has a lower and upper limits of 0 and CW as the success case, its pmf can be different from the one of a uniform random variable. However, we approximate it as a uniform random variable. As a result, the amount of time needed for DCF protocol to successfully transmit the first frame during T_i period given a s_{i-1} or f_{i-1} state for T_{i-1} are the same and equal to X. This approximation would have a light impact on the throughput computation since the sum between the first part of the backoff counter which occurs before the eNodeB-ON period and the second part of the backoff counter which occurs after the end of the eNodeB-ON period is a normal complete backoff. Indeed, if the eNodeB-ON period starts at the beginning of the backoff period or at the end, the next Wi-Fi frame will be transmitted exactly at the same time. More precisely, the time between the last frame sent before the eNodeB-ON period and the first frame sent after that period is $DIFS + eNodeB\text{-}ON + \delta * BFcounter_{unif(0,CW)} + DIFS$.

Finally, in the last case when the T_{i-1} period state is c_{i-1} (collision), the amount of time needed to successfully transmit the first frame during T_i can be represented by the following uniform random variable Y:

$$Y = DIFS + \delta * BFcounter_{unif(0,2*(CW+1)-1)} + Frame_{time} \quad (2)$$

As for all the next frames that follow the first one, the amount of time needed to successfully transmit any one of these frames can be easily represented by the same random variable X. In order to compute the transition probabilities, we need to determine when the last AP transmission is interrupted by the starting of the eNodeB-ON period. To do so, it is necessary to know how much Wi-Fi frames are sent during T_i period. Let N be the random variable that counts the number of frames which could be transmitted during any T_i period. For any given $N = n$, the first $n-1$ frames will be successfully transmitted and the n^{th} frame could be a collision, frozen or successful frame as shown in Figure 1. According to the above analysis and equations (1) and (2), the total time needed to transmit successfully n frames during any T_i period is the sum of n uniformly distributed random variables. This sum is equal to $\sum_{j=1}^{n} x_j$ if the state of the previous T_{i-1} period is s_{i-1} or f_{i-1}, and it is equal to $y + \sum_{j=2}^{n} x_j$ if the state of the previous T_{i-1} period is c_{i-1}. The first mentioned sum constitues an ordinary renewal process ($n \geq 0$), while the second sum is a delayed renewal process because the first random variable in the sum has a different distribution. The pmf of N depends on the state of T_{i-1} period. However, in any case, it is clear that N is a stopping time with respect to the sequence $\{x_1, x_2, x_3, \cdots\}$ or $\{y, x_2, x_3, \cdots\}$. Consequently, the conditional probability of sending n frames during any T_i period given that the state of T_{i-1} is s_{i-1} can be written as [13].

$$\begin{aligned} Pr\{N = n \mid s_{i-1}\} = Pr\{\sum_{j=1}^{n-1} x_j + DIFS + \delta < T_i\} \\ - Pr\{\sum_{j=1}^{n} x_j + DIFS + \delta < T_i\} \end{aligned} \quad (3)$$

Here, the stopping condition is $\sum_{j=1}^{n} x_j > T_i - DIFS - \delta$. **Explanation.** This conditional probability corresponds to the number of sent frames regardless of what happens to the last sent frame before the end of the T_i period. As a matter of fact, in equation (3), the addition of the $DIFS + \delta$ period is necessary to cover the three cases, collision, frozen and successful as shown in Figure 1. Particularly, if eNodeB-ON starts at the end of the added $DIFS + \delta$ period, then this case corresponds also to n sent frames with the last one being successful. Remind that the backoff counter is decremented at the end of the time slot δ. Hence, a full $DIFS + \delta$ period must be added. This probability can be computed exactly by using the pmf of the sum of n uniform random variables which is the n-fold convolution of individual pmfs.

Next, we determine the transition probabilities to s_i, f_i and c_i states with n transmitted frames during T_i given s_{i-1} state in the previous T_{i-1} as follows

$$Pr\{s_i, n \mid s_{i-1}\} = Pr\{\sum_{j=1}^{n} x_j < T_i \leq \sum_{j=1}^{n} x_j + DIFS + \delta\} \quad (4)$$

$$Pr\{f_i, n \mid s_{i-1}\} = Pr\{\sum_{j=1}^{n-1} x_j + DIFS + \delta < T_i < \sum_{j=1}^{n} x_j - Frame_{time}\} \quad (5)$$

$$Pr\{c_i, n \mid s_{i-1}\} = Pr\{\sum_{j=1}^{n} x_j - Frame_{time} \leq T_i \leq \sum_{j=1}^{n} x_j\} \quad (6)$$

For a given T_i period, N has an upper bound $nmax$, which means that $Pr\{N > nmax\} = 0$, where $nmax = \lceil T_i/xmin \rceil$ with $xmin = DIFS + Frame_{time}$. Hence, the transition probability to c_i state given s_{i-1} state is expressed as

$$Pr\{c_i \mid s_{i-1}\} = \sum_{n=1}^{nmax} Pr\{c_i, n \mid s_{i-1}\} \quad (7)$$

Similarly, we can compute all other transition probabilities. In particular, the conditional probability of sending n frames and the conditional transition probabilities to s_i, f_i and c_i states with n sent frames during T_i given f_{i-1} state in the previous T_{i-1} are the same as equations (3), (4), (5), (6) and (7). As for the conditional probability of sending n frames and the conditional transition probabilities to s_i, f_i and c_i states with n sent frames during T_i given c_{i-1} state in the previous T_{i-1}, they are obtained similarly except that $\sum_{j=1}^{n} x_j$ is replaced by $y + \sum_{j=2}^{n} x_j$.

Using the transition probabilities, we can deduce the probability of occurrence of each state at multiples of M, $\forall i \in (1, \cdots, M)$.

$$\pi(s_i) = Pr\{s_i \mid c_{i-1}\} * \pi(c_{i-1}) + Pr\{s_i \mid f_{i-1}\} * \pi(f_{i-1}) + Pr\{s_i \mid s_{i-1}\} * \pi(s_{i-1})$$

$$\pi(c_i) = Pr\{c_i \mid c_{i-1}\} * \pi(c_{i-1}) + Pr\{c_i \mid f_{i-1}\} * \pi(f_{i-1}) + Pr\{c_i \mid s_{i-1}\} * \pi(s_{i-1})$$

$$\pi(f_i) = Pr\{f_i \mid c_{i-1}\} * \pi(c_{i-1}) + Pr\{f_i \mid f_{i-1}\} * \pi(f_{i-1}) + Pr\{f_i \mid s_{i-1}\} * \pi(s_{i-1})$$

$$\pi(s_i) + \pi(c_i) + \pi(f_i) = 1 \quad (8)$$

We remind here again that $i-1$ refers to M if $i = 1$.

Finally, we can compute the probability of collision P_C seen by any frame during a duty cycle period consisting of M different T_i periods

$$P_C = \frac{E[collided\, frames\, during\, duty\, cycle\, period]}{E[sent\, frames\, during\, duty\, cycle\, period]} = \left(\sum_{i=1}^{M} E[C \text{ in } T_i]\right) / \left(\sum_{i=1}^{M} E[N \text{ in } T_i]\right) \quad (9)$$

The numerator of (9) is equal to the expected value of collided frames C in T_i period. As only the n^{th} frame during T_i period would face a collision, we can easily compute it as follows

$$E[C \text{ in } T_i] = \pi(c_i) \quad (10)$$

Next, we compute the expected value of N sent frames in T_i period

$$E[N \text{ in } T_i] = E[N] - E[F \text{ in } T_i] \quad (11)$$

Where $E[N]$ is the expected values of N sent frames regardless of what happens to the last sent frame before the end of the T_i period

$$E[N] = E[N \mid c_{i-1}] * \pi(c_{i-1}) + E[N \mid f_{i-1}] * \pi(f_{i-1}) + E[N \mid s_{i-1}] * \pi(s_{i-1}) \quad (12)$$

Hence, the conditional expected values of N such that c_{i-1}, f_{i-1} or s_{i-1} are respectively

$$E[N \mid c_{i-1}] = \sum_{n=1}^{nmax} n * Pr\{N = n \mid c_{i-1}\} \quad (13)$$

$$E[N \mid f_{i-1}] = \sum_{n=1}^{nmax} n * Pr\{N = n \mid f_{i-1}\} \quad (14)$$

$$E[N \mid s_{i-1}] = \sum_{n=1}^{nmax} n * Pr\{N = n \mid s_{i-1}\} \quad (15)$$

Finally, $E[F \text{ in } T_i]$ is the expected value of frozen frames F in T_i period which is necessary to not count it in $E[N \text{ in } T_i]$ (See Figure 1 case 2). It is calculated as follows

$$E[F \text{ in } T_i] = \pi(f_i) \quad (16)$$

Discussion. The probability of collision in (9) quantifies the impact of LTE-U TDM scheme on the Wi-Fi downlink transmissions while assuming one access point AP. The collisions occur exactly at the end of each T_i period. Let us consider the downlink and uplink Wi-Fi transmission with a finite number of Wi-Fi stations. Bianchi [14] and Altman *et al.* [15] have modeled the exponential behavior of the random backoff time to tie up between the probability of collision and the probability that a station transmits in a randomly chosen time slot. They have shown the intuitive result that when the number of Wi-Fi stations increases, the probability of collision increases as well, which leads to decreasing the probability that a station transmits in a randomly chosen time slot. Consequently, the probability of having the Wi-Fi stations not transmitting at the end of each T_i period is increased compared to one station. Indeed, these stations would be in a backoff period or colliding. As a result, our probability of collision on Wi-Fi transmission provides an *upper bound* of the impact caused by LTE-U TDM scheme on a Wi-Fi network with more than one station transmitting over the uplink. Note also that our model is extendible to take into consideration possible capture effects when Wi-Fi is able to receive correctly a frame even in case of collision [16]. It can be done by reducing adequately the transition probabilities from the collision state.

B. Downlink Wi-Fi Throughput

Let Γ be the downlink saturation throughput defined as the fraction of time the channel is used for successful transmissions. We express Γ as

$$\Gamma = \frac{E[successful\, frames\, during\, duty\, cycle\, period]}{duty\, cycle\, period\, time} = \frac{\sum_{i=1}^{M} E[S \text{ in } T_i]}{duty\, cycle\, period\, time} \quad frames/second \quad (17)$$

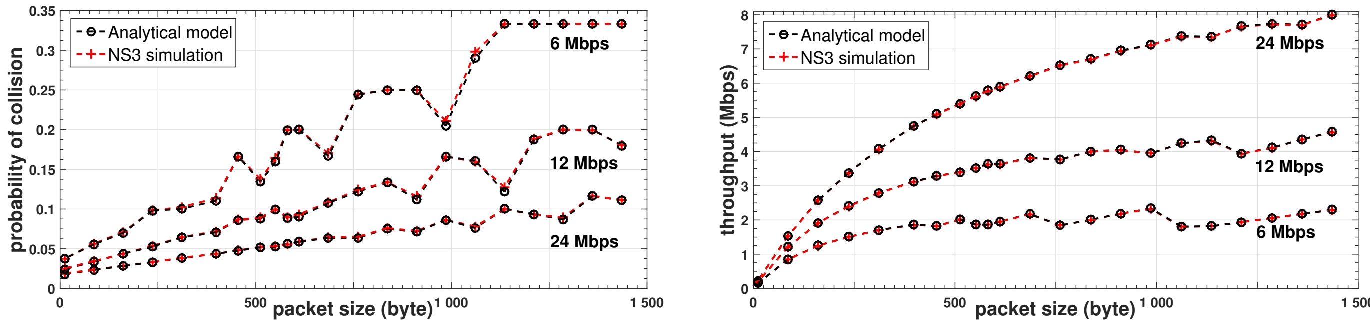

(a) Three different rates 6, 12 and 24 Mbps

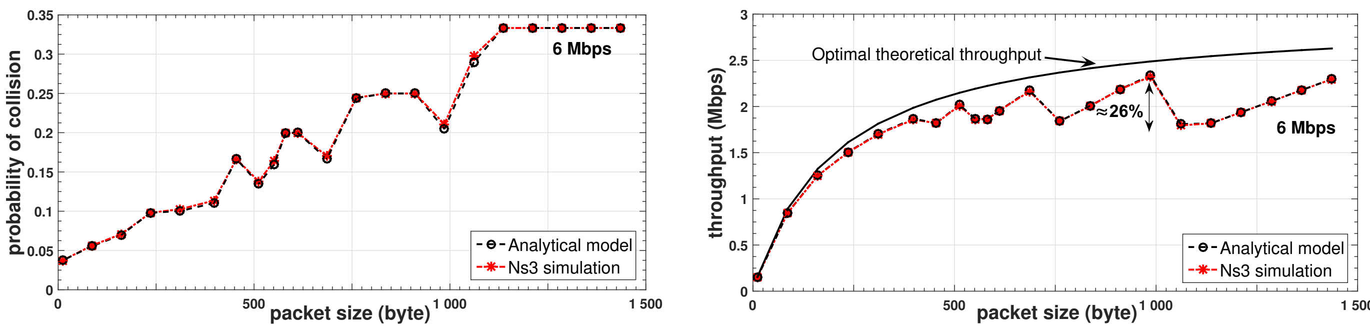

(b) Zoom in the 6 Mbps case

Fig. 3: (Left To Right) The probability of collision and throughput versus different packet size for 5x0 ON/OFF pattern

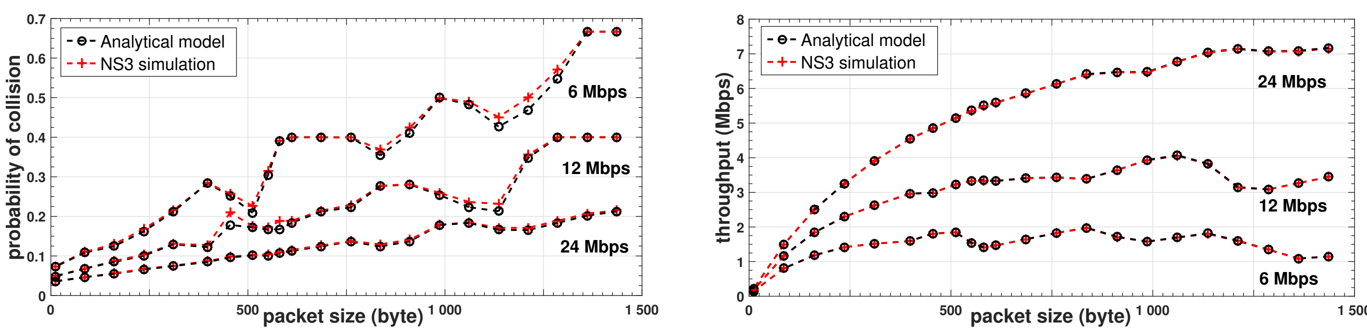

Fig. 4: (Left To Right):The probability of collision and throughput versus different packet size for 3x2 ON/OFF pattern

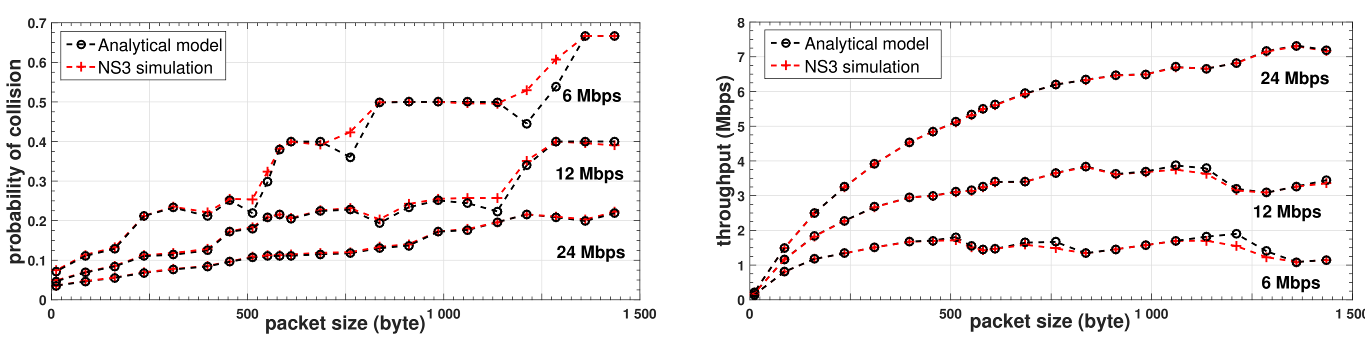

Fig. 5: (Left To Right) The probability of collision and throughput versus different packet size for 4x1 ON/OFF pattern

For the expected value of successful frames S in any T_i period, we can use the fact that during the T_i period, the first $n-1$ frames are sent successfully. However, the last one is only successful with probability $\pi(s_i)$. Hence,

$$E[S \text{ in } T_i] = E[N] - 1 + \pi(s_i) \tag{18}$$

Particularly, if the eNodeB-ON periods are equal to eNodeB-OFF periods so that the bandwidth is shared "equally" between LTE-U and Wi-Fi, the expression of the throughput becomes

$$\Gamma = \frac{\sum_{i=1}^{M} (E[N] - 1 + \pi(s_i))}{2 \times \sum_{i=1}^{M} T_i} \quad frames/second \tag{19}$$

Equation (19) provides the maximum throughput that is obtained on the downlink transmissions towards the users of the Wi-Fi access point. This throughput is of course lower than the Wi-Fi bandwidth divided by 2 due to LTE impact as we shall see in the next section.

IV. MODEL VALIDATION AND RESULTS

To validate our analytical model, we have simulated the interaction between LTE-U and Wi-Fi using NS3 simulator. As this paper aims to quantify the impact of LTE-U TDM scheme on the Wi-Fi MAC DCF protocol and since 802.11a/n/ac have similar definitions of the MAC layer, we choose the implementation of IEEE 802.11a standard in the simulator. We simulate a Wi-Fi access point transmitting continuously to its users. We implement a new model to simulate eNodeB-ON and OFF periods. During eNodeB-ON periods, a signal is generated so that Wi-Fi AP detects a busy channel if it is in sensing periods, otherwise the signal causes interferences with Wi-Fi transmissions leading to collisions and the frame is lost.

Simulation time	200 s
Payload packet	11 $\sim$ 1436 bytes
ACK packet	14 bytes
UDP header	8 bytes
Network header	20 bytes
MAC header	36 bytes
Channel bit rate	6, 12 and 24 Mbps
Channel bandwidth	20 MHz
Slot time (δ)	9 μs
SIFS	16 μs
DIFS	34 μs

TABLE I: Wi-Fi transmission parameters used in the comparison between NS3 simulations and the analytical model

Wi-Fi parameters used to obtain the numerical results for both the analytical model and the NS3 simulation are those specified by default in the IEEE 802.11a standard, as reported in Table I. We have used in the simulation runs a Wi-Fi channel with a bit rate equals to 6, 12 or 24 Mbps corresponding to different Modulation and Coding Schemes (MCS), i.e. BPSK, QPSK, 16QAM. The packet payload varies from 11 bytes to 1436 bytes. The Wi-Fi probability of collision obtained by simulation is computed by dividing the number of collided frames (i.e. retransmitted frames) over the total number of transmitted frames at the MAC layer. The simulation throughput is obtained by counting the total successfully received frames during the simulation time at the application layer. For a fixed set of parameters, we repeat the simulations 3 times. Confidence intervals are too small to be drawn on the plots. We remark that each simulation run can last for several hours especially for small packet sizes since the number of events in this case is very high.

Without losing the generality of our analysis, the LTE-U transmission duty cycle period is fixed to 10 ms corresponding to LTE frame duration with duty cycle percentage of 50% so that LTE-U leaves somewhat an "equal" share to Wi-Fi. We vary the distribution of the ON/OFF transmission periods of LTE-U inside the duty cycle. First, LTE-U transmission is activated for 5 ms then deactivated for the rest of LTE frame duration. This configuration refers to 5x0 ON/OFF pattern. Second, LTE-U transmission is activated for 3 ms at the beginning of the duty cycle, then deactivated for same amount of time before it is reactivated again for 2 ms. Consequently, the Wi-Fi AP gets two disjoint transmission opportunities in the same LTE frame to access the channel. This configuration refers to 3x2 ON/OFF pattern. Third, we consider another LTE-U transmission pattern similar to the previous one except we replace 3 ms by 4 ms, and we replace 2 ms by 1ms to get a 4x1 ON/OFF pattern.

A. Comparison With Simulation Results

Figure 3 shows that the analytical results for both the probability of collision and throughput are highly accurate with the simulation results for 6, 12 and 24 Mbps when the LTE-U transmission pattern is 5x0 ON/OFF. Especially, for 6 Mbps, the model follows exactly any abrupt fluctuation of the simulation results as shown in Figure 3b. As Wi-Fi access the channel for the half of the time with 6 Mbps, the optimal theoretical throughput experienced by Wi-Fi in case of full synchronization with LTE-U (i.e. without collision with LTE-U) is also shown in Figure 3b. Evidently, collisions degrade the throughput by a non-marginal amount.

Figure 4 relative to the 3x2 ON/OFF pattern, shows a slight difference between the analytical model and the simulation results especially for the rate of 6 Mbps. This is explained by the assumption made in the model that after a collision at the end of a T_i period, the retransmitted frame at the beginning of the next T_i period does not face a collision. This assumption is rarely violated for some packet sizes during the 2 ms period.

Figure 5 confirms that our analytical model is still robust even if the previous mentioned assumption is not valid. Actually, the assumption is violated for a larger number of packet sizes in case of 6 and 12 Mbps rate and the small period of 1 ms. As a result, such scenario can not be modeled by our Markovian chain whereas it still can capture globally the probability of collision and the throughput behavior. In contrast, using a rate of 24 Mbps fulfill our assumption and thus the analytical model results coincide again with the simulation results. Note that 6 Mbps is the lowest rate defined in the IEEE 802.11 standard.

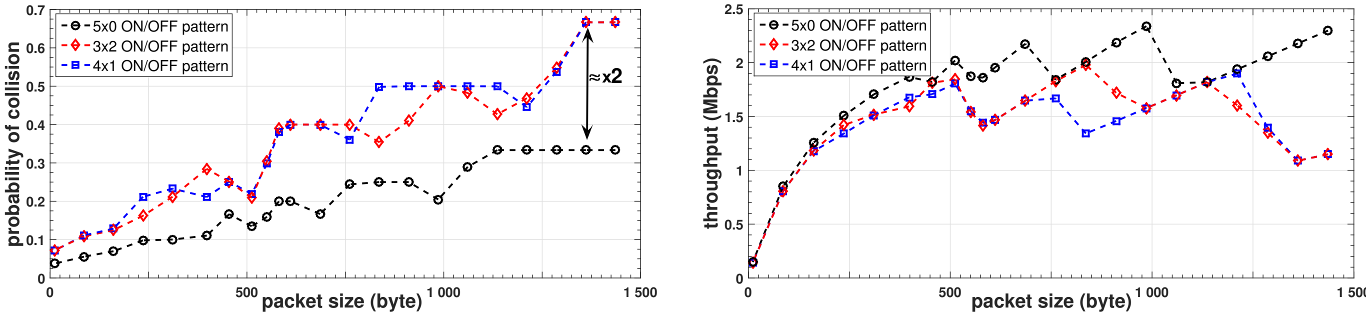

(a) 6 Mbps

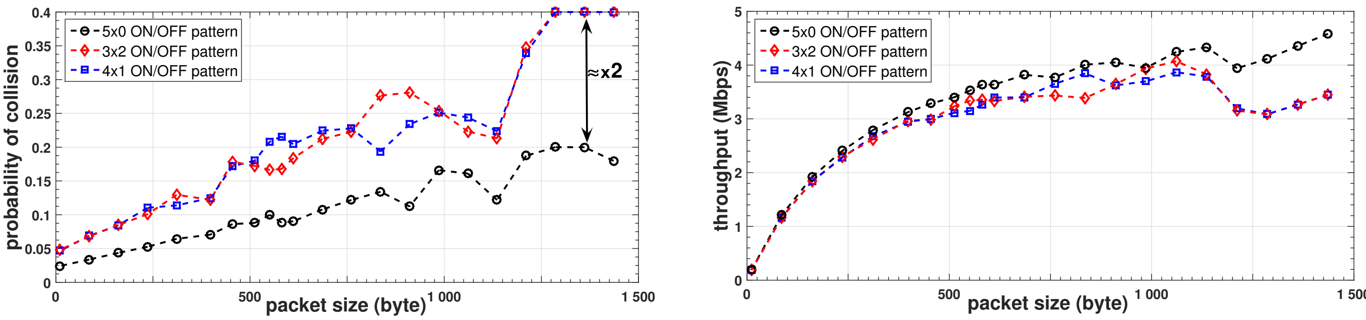

(b) 12 Mbps

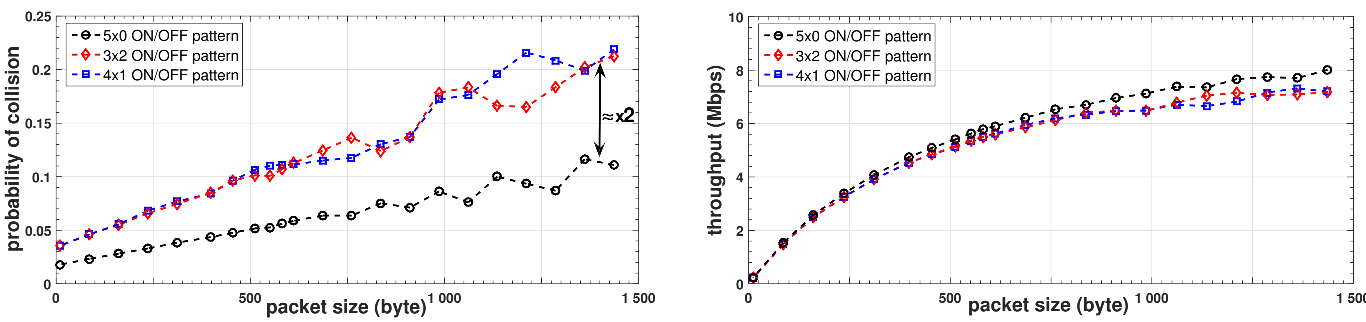

(c) 24 Mbps

Fig. 6: Comparison of the three ON/OFF patterns with different rates

B. Analyzing LTE-U Impact on Wi-Fi

First of all, the impact of LTE-U on Wi-Fi performance in terms of probability of collision and downlink throughput can be observed clearly when the total number of Wi-Fi packets that can be sent during a duty cycle period is relatively small. As a matter of fact, equation (9) shows that for a large number of sent packets by Wi-Fi during a duty cycle, the numerator will be small compared to the denominator, especially that only the last Wi-Fi packet in a T_i period can be lost. The average number of sent packets depends on the eNodeB-OFF length, the packet size and the Wi-Fi bit rate. For instance, the larger the bit rate, the lower the impact of LTE-U on Wi-Fi. Also, if the bit rate is small, then the impact is reduced when the packet size is small enough (Figure 3b). However, reducing the packet size does not necessarily increase the performance because a small packet size incurs more overhead.The tradeoff between a small packet size that reduces the collision probability and a large packet size that reduces the overhead becomes tricky. According to Figure 3b, if the rate of Wi-Fi is 6 Mbps, then a judicious choice of the packet size must be made to maximize the throughput. This packet size is computed easily through our proposed model.

More precisely, with a small packet size, the probability of collision has a positive linear relationship over the packet size but after a specific packet size, the probability of collision shows some ripples which depends drastically on the value of each packet size. For 24 Mbps, we observe the same behavior of the probability of collision except that the ripples appear from larger packet sizes. Accordingly, the throughput curves reflect the same behavior. For 6 Mbps, throughput ripples are so much sharp that may cause loosing up to 26% of throughput compared to the maximum. In contrast, for 24 Mbps, throughput ripples are negligible. Ripples are explained by the variability of the backoff periods which is not significant if the air frame time is large. In other words, the random part in X becomes small compared to the constant part (see equation

(1)). In this case, some periodic behavior appears where the number of Wi-Fi sent frames during the eNodeB-OFF period stays the same while increasing the frame size. As a matter of fact, interrupting the last frame in the eNodeB-OFF period at the beginning of the frame or at its end does not change the number of previous sent frames.

Globally, the above observations about the 5x0 ON/OFF pattern apply for 3x2 and 4x1 ON/OFF pattern except that values are different (Figure 6). For instance, with 6 Mbps the packet sizes that approach the optimal theoretical throughput are different for the 3x2 and 4x1 ON/OFF pattern and throughput ripples causes to loosing respectively up to 43% and 40% of throughput compared to the maximum. In contrast, for both 12 and 24 Mbps the throughput for both pattern are nearly the same.

Figure 6 shows, using our analytical model, that 5x0 ON/OFF pattern has a better performance than 3x2 and 4X1 ON/OFF pattern for both probability of collision and throughput and for all different data rates. That could be explained by the probability of collision of the 3x2 or 4X1 ON/OFF pattern is approximately doubled compared to 5x0 ON/OFF pattern for almost all packet sizes because LTE-U transmission interrupts Wi-Fi transmission twice over each duty cycle period. Consequently, 5x0 ON/OFF pattern throughput is always better than the 3x2 and 4x1 ON/OFF patterns. Nevertheless, it is intuitive that for 5X0 ON/OFF pattern, the Wi-Fi packets may have higher delays to access the channel in comparison with the 3X2 and 4X1 ON/OFF pattern. This raises the tradeoff issue between the delay and the throughput experienced by Wi-Fi.

V. Conclusions and Future Work

This paper quantifies the impact of LTE-U on Wi-Fi downlink performance when a TDM sharing scheme is deployed by LTE. Using an efficient analytical model that captures the exact periodic behavior of LTE-U, the impact has been evaluated in terms of probability of collision between the two systems. This probability of collision represents an upper bound of the negative impact when Wi-Fi uplink and downlink transmissions are active together. Accordingly, the maximum throughput that can be achieved by Wi-Fi has been evaluated. Comparing our model results to those obtained by NS3 simulations validates both our analytical model and the new implemented model of IEEE 802.11 MAC in NS3 for the research community.

Performance analyses show that LTE-U must share the channel with Wi-Fi intelligently to reduce the negative impact on Wi-Fi due to collisions. In other words, it is not enough to share equally the channel by deploying a 50% ON/OFF duty cycle. How the channel is shared inside the duty cycle is an important factor as well. Relying on our model, we can measure exactly the performance degradation for any TDM scheme. Henceforth, it is possible to find the required compensation that makes the sharing equal, by increasing the access time available to Wi-Fi during each TDM duty cycle. Thus, LTE-U can recover adequately the disuse of the Wi-Fi CSMA/CA scheme, On the other hand, Wi-Fi can better protect itself from the negative impact of LTE-U by frame buffering and aggregation so that a suitable air frame size is used, especially with low data rates.

Currently, we are considering the case where multiple Wi-Fi access points are competing for the spectrum in presence of LTE-U. Two modeling concepts may be applied here. The first one is extending the model of Bianchi [14] or Altman *et al.* [15]. The second is to extend our model by computing for instance the distribution of the inter-arrival time between successive Wi-Fi frames. Initial results show that, regardeless of the adopted approch, modeling Wifi network as a renewal process proposed in this paper is prerequisite to study precisly the interaction between the two systems.

References

[1] Cisco, "Cisco visual networking index: Global mobile data traffic forecast update 2014–2019," 2015.

[2] ETSI EN, "301 893 v1.7.1 (2012-06)," 2012.

[3] Q. Research, "Lte in unlicensed spectrum: Harmonious coexistence with wi-fi," 2014.

[4] C. Chen, R. Ratasuk, and A. Ghosh, "Downlink performance analysis of lte and wifi coexistence in unlicensed bands with a simple listen-before-talk scheme," in *Vehicular Technology Conference (VTC Spring), 2015 IEEE 81st*. IEEE, 2015, pp. 1–5.

[5] F. Abinader Jr, E. P. Almeida, F. S. Chaves, A. M. Cavalcante, R. D. Vieira, R. C. Paiva, A. M. Sobrinho, S. Choudhury, E. Tuomaala, K. Doppler *et al.*, "Enabling the coexistence of lte and wi-fi in unlicensed bands," *Communications Magazine, IEEE*, vol. 52, no. 11, pp. 54–61, 2014.

[6] NS3, "Official website." [Online]. Available: http://www.nsnam.org

[7] E. Almeida, A. M. Cavalcante, R. C. Paiva, F. d. S. Chaves, F. Abinader, R. D. Vieira, S. Choudhury, E. Tuomaala, and K. Doppler, "Enabling lte/wifi coexistence by lte blank subframe allocation," in *Communications (ICC), 2013 IEEE International Conference on*. IEEE, 2013, pp. 5083–5088.

[8] L. A. Joey Padden, "Wi-fi vs. duty cycled lte: A balancing act," 2014. [Online]. Available: http://www.cablelabs.com/wi-fi-vs-duty-cycled-lte/

[9] A. Cavalcante, E. Almeida, R. D. Vieira, F. Chaves, R. Paiva, F. Abinader, S. Choudhury, E. Tuomaala, and K. Doppler, "Performance evaluation of lte and wi-fi coexistence in unlicensed bands," in *Vehicular Technology Conference (VTC Spring), 2013 IEEE 77th*. IEEE, 2013, pp. 1–6.

[10] F. d. S. Chaves, E. P. Almeida, R. D. Vieira, A. M. Cavalcante, F. Abinader, S. Choudhury, and K. Doppler, "Lte ul power control for the improvement of lte/wi-fi coexistence," in *Vehicular Technology Conference (VTC Fall), 2013 IEEE 78th*. IEEE, 2013, pp. 1–6.

[11] F. Chaves, A. Cavalcante, E. Almeida, F. Abinader Jr, R. Vieira, S. Choudhury, and K. Doppler, "Lte/wi-fi coexistence: Challenges and mechanisms."

[12] J. Jun, P. Peddabachagari, and M. Sichitiu, "Theoretical maximum throughput of ieee 802.11 and its applications," in *Network Computing and Applications, 2003. NCA 2003. Second IEEE International Symposium on*. IEEE, 2003, pp. 249–256.

[13] S. M. Ross, *Introduction to probability models*. Academic press, 2014.

[14] G. Bianchi, "Performance analysis of the ieee 802.11 distributed coordination function," *Selected Areas in Communications, IEEE Journal on*, vol. 18, no. 3, pp. 535–547, 2000.

[15] A. Kumar, E. Altman, D. Miorandi, and M. Goyal, "New insights from a fixed point analysis of single cell ieee 802.11 wlans," in *INFOCOM 2005. 24th Annual Joint Conference of the IEEE Computer and Communications Societies. Proceedings IEEE*, vol. 3. IEEE, 2005, pp. 1550–1561.

[16] K. Leentvaar and J. Flint, "The capture effect in fm receivers," *IEEE Transactions on Communications*, vol. 24, no. 5, pp. 531–539, May 1976.